Journal of Hydroscience and Hydraulic Engineering
Vol. 7, No. 2, March, 1990, 61-68

INFLUENCE OF THE DENSITY AND VELOCITY PROFILES ON CALCULATED INSTABILITY CHARACTERISTICS IN AN INVISCID TWO-LAYER SHEAR FLOW

By

Shuzo NISHIDA

Associate Professor, Department of Civil Engineering
Hachinohe Institute of Technology, Hachinohe 031, Japan

and

Shizuo YOSHIDA

Associate Professor, Department of Engineering Science
Hokkaido University, Sapporo 060, Japan

SYNOPSIS

The instability of an inviscid two-layer flow with a hyperbolic-tangent velocity profile is investigated using the linear stability theory to clarify the influence of the density and velocity profiles on calculated instability characteristics. The numerical results show that there is a region of stationary unstable modes at low Richardson number R_i and only one neutral curve at low wavenumber α in the (α, R_i) plane, so that the flow is always unstable for α larger than about $R_i/2$. Moreover, it was found that the appearance of a neutral curve at high α obtained in the models of Holmboe and Hazel is due to the discontinuity of vorticity profile and the continuity of density profile, respectively.

INTRODUCTION

Many studies have been made on the instabilities of stratified shear flows to make clear critical conditions for generation of turbulence or internal waves. One of the important results is that inviscid shear flows with a sharp density interface are always unstable for some wavenumbers, while flows with an unbounded layer, *i.e.* the continuity of density profile, are unstable only in the region of low Richardson number, $J<1/4$ (see Drazin & Howard[2]).

Hazel[4] analyzed the shear-induced instability numerically under the different sized vertical scales for the density and velocity profiles, and explained the difference in instability characteristics between stratified flows of smooth and abrupt density profile by using a chart of local Richardson number profile. According to this results, there are many similar points, *e.g.* shape of neutral curves, between Hazel's numerical results and Holmboe's results[5] for the flow with a sharp interface. However, a close examination shows clear differences between their results, *e.g.* stationary unstable mode.

In this paper we numerically investigate the instability of a density two-layer flow with a hyperbolic-tangent velocity profile, as a combination of Hazel's and Holmboe's models, with the intention of clarifying the influence of flow modeling on the instability analysis.

FORMULATION OF THE PROBLEM

We consider a two-dimensional incompressible inviscid parallel flow with a velocity profile $U^*=V\cdot\tanh(y^*/l)$ which is a statically stable two-layer system with densities of

fluids ρ_1 and ρ_2 ($\rho_1<\rho_2$), in the upper and lower layers, respectively. Assuming the fluids are fresh water and saline water, we can ignore the surface tension at the interface. If we take a dimensionless stream function of disturbance $\phi(y)\exp\{i\alpha(x-Ct)\}$, the well-known Rayleigh equation for each layer is deduced after linearization:

$$\phi_1''-\left\{\frac{U''}{(U-C)}+\alpha^2\right\}\phi_1=0$$
$$\phi_2''-\left\{\frac{U''}{(U-C)}+\alpha^2\right\}\phi_2=0 \qquad (1)$$

where U is the dimensionless velocity profile given by $U=\tanh(y)$, $C\,(=C_r+iC_i)$ the dimensionless complex phase velocity, α the dimensionless wavenumber and primes denote differentiation with respect to the dimensionless height y.

According to the continuity of displacement and pressure across the interface, boundary conditions can be obtained as

$$\phi_1=0 \quad (y=+\infty)$$
$$\phi_2=0 \quad (y=-\infty)$$
$$\phi_1=\phi_2 \quad (y=0) \qquad (2)$$
$$\gamma(U-C)\phi_1'-\gamma U'\phi_1=(U-C)\phi_2'-U'\phi_2-\frac{R_i}{(U-C)}\phi_2 \quad (y=0)$$

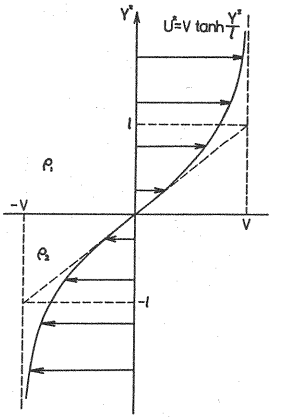

Fig.1 Flow model

where $\gamma=\rho_1/\rho_2$ is the density ratio, $R_i=(1-\gamma)gl/V^2$ the Richardson number, and g the gravitational acceleration. Since Eqs.(2) show that effects of density difference on the stability can be disregarded, except the term containing g, we let γ be a constant value of 0.99 (Boussinesq approximation). Then we obtain the eigenvalue equation from the boundary conditions,

$$det[\Delta(\alpha, C; R_i)]=0 \qquad (3)$$

ANALYSIS AND NUMERICAL SCHEME

Substituting the dimensionless velocity profile $U=\tanh(y)$ into the Rayleigh equation, and transforming using $\zeta=\tanh(y)$, we can get the following equation (Tominaga[10]).

$$\frac{d^2\phi}{d\zeta^2}-\frac{2\zeta}{1-\zeta^2}\frac{d\phi}{d\zeta}+\left[\frac{2\zeta}{(\zeta-C)(1-\zeta^2)}-\frac{\alpha^2}{(1-\zeta)^2}\right]\phi=0 \qquad (4)$$

Furthermore, transforming Eq.(4) using

$$\phi=(1-\zeta^2)^{\alpha/2}(\zeta-C)\psi\,, \qquad \zeta=(1+\xi)/2 \qquad (5)$$

we obtain the equation as follows:

$$\frac{d^2\psi}{d\xi^2}+\left(\frac{\gamma_1}{\xi}+\frac{\delta_1}{\xi-1}+\frac{\alpha_1+\beta_1-\gamma_1-\delta_1+1}{\xi-a_1}\right)\frac{d\psi}{d\xi}+\frac{\alpha_1\beta_1(\xi-q_1)}{\xi(\xi-1)(\xi-a_1)}\psi=0 \qquad (6)$$

where

$$\alpha_1=\alpha,\ \beta_1=\alpha+3,\ \gamma_1=\alpha+1,\ \delta_1=\alpha+1,\ a_1=(C+1)/2,\ q_1=(a_1\alpha+a_1+1)/(a_1+3) \qquad (7)$$

This equation is called Heun's equation (Bateman[1]), which has four singular points at $\xi=0$, a_1, 1, and ∞. Two independent solutions in the vicinity of $\xi=0$ are obtained as follows:

$$\psi_1=F(a_1;\ \alpha_1, \beta_1, \gamma_1, \delta_1;\ q_1;\ \xi)=\sum_{n=0}^{\infty}A_n\xi^n$$
$$A_0=1,\ A_1=\frac{\alpha_1\beta_1q_1}{a_1\gamma_1},$$
$$A_{n+1}=\frac{1}{a_1(n+1)(\gamma_1+n)}[\{(a_1+1)n^2+(\gamma_1+\delta_1-1)a_1n+(\alpha_1+\beta_1-\delta_1)n$$
$$+\alpha_1\beta_1q_1\}A_n+(\alpha_1+n-1)(\beta_1+n-1)A_{n-1}] \qquad (8)$$

$$\psi_2=\xi^{1-\gamma_1}F(a_1;\ \alpha_1-\gamma_1+1,\ \beta_1-\gamma_1+1,\ 2-\gamma_1,\ \delta_1;\ \frac{\alpha_1\beta_1q_1-(1-\gamma_1)\{\gamma_1-\alpha_1-\beta_1-(a_1-1)\delta_1-1\}}{(\alpha_1-\gamma_1+1)(\beta_1-\gamma_1+1)};\ \xi)$$

One of the independent solutions in the vicinity of $\xi=a_1$ incorporates a log term as follows:

$$\begin{aligned}
&\psi_3=F\Big(\frac{a_1-1}{a_1};\ \alpha_1,\ \beta_1,\ \alpha_1+\beta_1-\gamma_1-\delta_1+1,\ \gamma_1;\ \frac{a_1-q_1}{a_1};\ \frac{a_1-\xi}{a_1}\Big)=\sum_{n=0}^{\infty}B_n\Big(\frac{a_1-\xi}{a_1}\Big)^n\\
&\psi_4=k\psi_3\log(\xi-a_1)+(\xi-a_1)^{-1}\sum_{n=0}^{\infty}C_n(\xi-a_1)^n\\
&\quad k=\frac{(2a_1-1)}{a_1(a_1-1)B_0},\ C_0=1,\ C_1=0,\\
&\quad C_{n+1}=\frac{-1}{(a_1-1)(n+1)a_1n}[(2n+\alpha_1+\beta_1-4)B_{n-2}+(2a_1-1)(2n+\alpha_1)B_{n-1}\\
&\qquad +a_1(a_1-1)(2n+1)B_n+\{(n-2)(n-3)+(n-2)(\alpha_1+\beta_1+1)+\alpha_1\beta_1\}C_{n-1}\\
&\qquad +\{(2a_1-1)(n-1)(n+\alpha_1+1)+\alpha_1\beta_1\ (a_1-q_1)\}C_n]
\end{aligned}\tag{9}$$

and independent solutions in the vicinity of $\xi=1$ are obtained by parameter conversion as follows:

$$\begin{aligned}
&\psi_5=F(1-a_1;\ \alpha_1,\ \beta_1,\ \delta_1,\ \gamma_1;\ 1-q_1;\ 1-\xi)\\
&\psi_6=(1-\xi)^{1-\delta_1}F(1-a_1;\ \alpha_1-\delta_1+1,\ \beta_1-\delta_1+1,\ 2-\delta_1,\ \gamma_1;\\
&\qquad\qquad \frac{(1-q_1)\alpha_1\beta_1-(1-\delta_1)(\delta_1-\alpha_1-\beta_1+a_1\gamma_1-1)}{(\alpha_1-\delta_1+1)(\beta_1-\delta_1+1)};\ 1-\xi)
\end{aligned}\tag{10}$$

Then, the solution of Eq.(6) near each singular point is represented as follows:

$$\begin{aligned}
&\phi=(1-\xi)^{\alpha/2}(\xi-a_1)[P_1\psi_1+P_2\psi_2] \qquad \text{for}\ \ \xi=0\\
&\phi=(1-\xi)^{\alpha/2}(\xi-a_1)[P_3\psi_3+P_4\psi_4] \qquad \text{for}\ \ \xi=a_1\\
&\phi=(1-\xi)^{\alpha/2}(\xi-a_1)[P_5\psi_5+P_6\psi_6] \qquad \text{for}\ \ \xi=1
\end{aligned}\tag{11}$$

By using a_1 and ξ, the boundary conditions (2) are represented as follows:

$$\begin{aligned}
&\phi_1=0\quad(\xi=1)\\
&\phi_2=0\quad(\xi=0)\\
&\phi_1=\phi_2\quad(\xi=0.5)\\
&4\gamma(\xi-a_1)^2\frac{d\phi_1}{d\xi}-8\gamma(\xi-a_1)(1-\xi)\xi\phi_1=4(\xi-a_1)^2\frac{d\phi_2}{d\xi}-8(\xi-a_1)(1-\xi)\xi\phi_2-R_i\phi_2\quad(\xi=0.5)
\end{aligned}\tag{12}$$

Furthermore, denoting an upper solution and lower one at the inner boundary by ϕ_u and ϕ_l respectively, additional conditions of adjoining solutions in the domain of convergence are represented as follows:

$$\phi_u=\phi_l,\qquad \frac{d\phi_u}{d\xi}=\frac{d\phi_l}{d\xi}\tag{13}$$

From these conditions, we can obtain the simultaneous equations,

$$\begin{bmatrix} a_{11} & a_{12}\cdots\cdots \\ a_{21} & \\ \vdots & \vdots \\ \cdots\cdots & a_{66} \end{bmatrix}\begin{bmatrix} P_1 \\ \vdots \\ P_6 \end{bmatrix}=\Delta\cdot\begin{bmatrix} P_1 \\ \vdots \\ P_6 \end{bmatrix}=[0]\tag{14}$$

and the eigenvalue equation (3) can be found.

Because adjoining solutions were made to coalesce at the middle point of each overlap region to maintain the convergency of solutions, we obtained a matrix and an eigenvalue equation with different rank in each of the six regions of Howard's semicircle transformed into the a_1 plane. The matching points of solutions were determined as follows by considering the value of C for each of the six cases corresponding to regions of 1 to 6 in Fig.2.

(1) $\xi_i,\ \xi_1\ (\xi_1<\xi_i)$

(2) ξ_i, ξ_2 $(\xi_2<\xi_i)$
(3) ξ_i, ξ_2, ξ_3 $(\xi_2<\xi_i<\xi_3)$
(4) ξ_i, ξ_4, ξ_5 $(\xi_4<\xi_i<\xi_5)$
(5) ξ_i, ξ_4 $(\xi_4>\xi_i)$
(6) ξ_i, ξ_5 $(\xi_5>\xi_i)$

where ξ_i is the interface level, $\xi_i=0.5$ in the present case, and ξ_1 to ξ_5 are the levels defined as

$$\xi_1=(|a_1|+1-|1-a_1|)/2$$
$$\xi_2=(2R_e(a_1)-1+|a_1|)/2$$
$$\xi_3=(2-|1-a_1|)/2 \qquad (15)$$
$$\xi_4=|a_1|/2$$
$$\xi_5=(2R_e(a_1)+1-|1-a_1|)/2$$

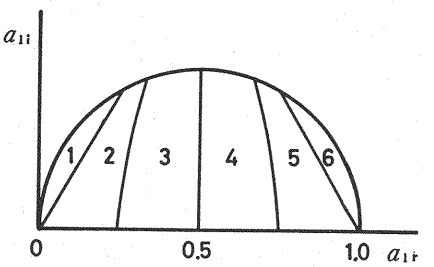

Fig.2 Howard's semicircle transformed into a_1 plane

The actual calculation was carried out by the following procedure. First, we calculate values of the real part D_r and the imaginary part D_i of the determinant of Eq.(3) for given R_i, α and the expected value of C, using ψ_1 to ψ_6 and their derivatives at the boundary. Next, iterating this calculation for C varied with a step size ΔC_r and ΔC_i, we draw $D_r=0$ and $D_i=0$ curves in the (C_r, C_i) plane. If the curves intersect, the value of C at the cross point is the eigenvalue. Furthermore, calculating with the above procedure taking ΔC_r and ΔC_i smaller near the C obtained, we can get the eigenvalue with higher accuracy.

RESULTS AND DISCUSSION

Stability Characteristics

Figures 3 and 4 show the phase velocity C_r and growth rate αC_i for $R_i=0.05$ and 1.0 respectively. By the calculations of C_r and αC_i for various α and R_i, we obtained the stability characteristics as shown in Fig.5 . We drew the αC_i curve in the shaded region matching the growth rate for $R_i=0$, although two different C_i's were obtained in this region due to a bifurcation of the αC_i curve (see Fig.3). The growth rate on the max. αC_i line in Fig.5 increases gradually with a decrease of R_i and reaches a local maximum at approximately $R_i=0.4$, and attains its maximum at $R_i=0$. The results at $R_i=0$ agree with Michalke's results[6] for homogeneous free shear flow. On the other hand, the phase velocity decreases gradually with the decrease of R_i and approaches about zero rapidly in the shaded region; the reason why C_r does not become exactly zero is that we took the γ to be not 1.0 but 0.99. However, the difference is $O(\varepsilon)$, where $\varepsilon=1-\gamma$; thus we will refer to this mode as the stationary mode hereafter.

As shown in Fig.5, the neutral curve at low α, expressed as $R_i=2\alpha$, was obtained, but the neutral curve was not found at high α within calculations ranging $0<\alpha<4$. This means that the flow is always unstable for α larger than $R_i/2$.

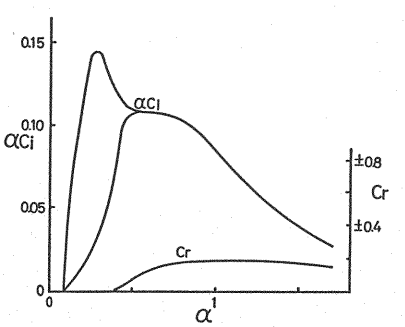

Fig.3 Phase velocity and growth rate for $R_i=0.05$

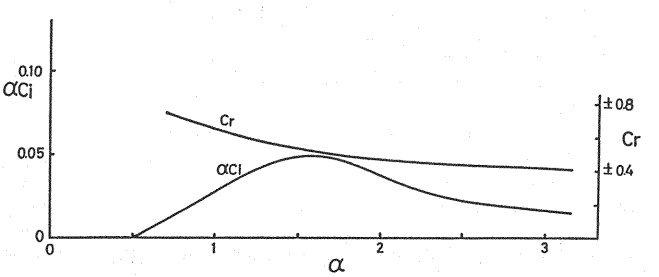

Fig.4 Phase velocity and growth rate for $R_i=1.0$

Comparison with Classical Kelvin-Helmholtz Instability

The stability of two-layer flow with constant densities ρ_1, ρ_2, and velocities U_1, U_2 in the upper and lower layer respectively is well-known as the classical Kelvin-Helmholtz problem, and the dispersion relation for the K-H problem is obtained as follows by Turner[11]:

$$C=\frac{\rho_1U_1+\rho_2U_2}{\rho_1+\rho_2}\pm\left\{\frac{g}{\alpha}\frac{\rho_2-\rho_1}{\rho_2+\rho_1}-\frac{\rho_1\rho_2}{(\rho_1+\rho_2)^2}(U_2-U_1)^2\right\}^{\frac{1}{2}} \tag{16}$$

In order to compare this relation with our results, we replace U_1, U_2 with V, $-V$, and use the assumption $(\rho_2-\rho_1)/\rho_2 \ll 1$. We can obtain the relation in the dimensionless form;

$$C=\pm\sqrt{\frac{R_i}{2\alpha}-1},\quad R_i=\frac{\varepsilon g l}{V_2} \tag{17}$$

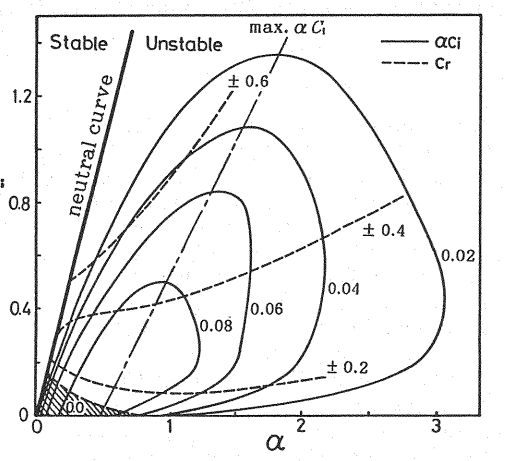

Fig.5 Stability characteristics of density two-layer flow with tanh velocity profile

We therefore obtain the condition of generation of unstable waves and their phase velocity as

$$R_i<2\alpha,\quad C_r=0 \tag{18}$$

Now, considering the case of $l\to 0$, *i.e.* $R_i\to 0$, in our model, the flow field approaches Kelvin-Helmholtz flow. Our results near $R_i=0$ show that the instability condition is represented by $R_i<2\alpha$ and that the phase velocity of unstable waves is nearly zero. These are therefore in agreement with the results of the Kelvin-Helmholtz problem. Note that flows with $R_i=0$ in our model represent not only homogeneous free shear flow (*i.e.* $\varepsilon=0$), but also Kelvin-Helmholtz flow (*i.e.* $l=0$).

Such agreement of stability characteristics near $R_i=0$ have also been found for the continuously stratified flows investigated by Miles & Howard[7], Thope[9] and others. Representing their results in terms of Richardson number R_i defined in the present study, we can obtain a neutral curve with $R_i=2\alpha$ and the phase velocity of unstable waves as zero. Drazin & Howard[2] have interpreted such general characteristics of instability by an α series expansion of the neutral stability solution.

Comparison with Other Studies

Holmboe[5] investigated the stability of a two-layer flow with the velocity profile

$$U=\begin{cases}y/|y| & (|y|>1)\\ y & (|y|<1)\end{cases} \tag{19}$$

and obtained the neutral curve shown in Fig.6. On the other hand, Hazel[4] numerically

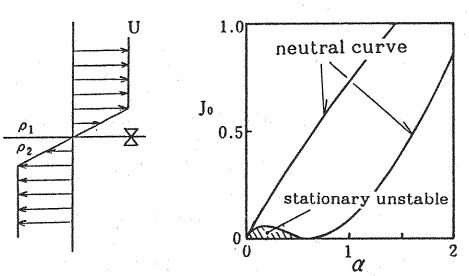

Fig.6 Flow model and resulting neutral curve by Holmboe

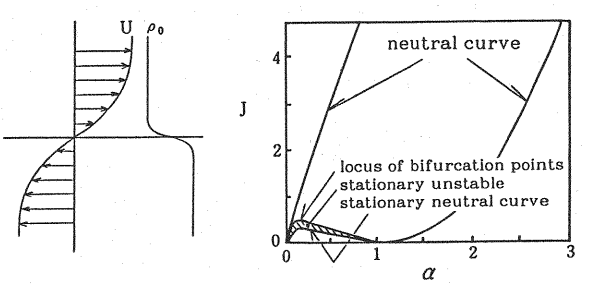

Fig.7 Flow model and resulting neutral curve by Hazel

investigated flows with velocity and density profile

$$U=\tanh y$$
$$\rho_0=\bar{\rho}\exp\left\{-\frac{\sigma}{R}\tanh(Ry)\right\} \tag{20}$$

and obtained the results for the case of R=5 as shown in Fig.7, where R is the ratio of the scale of velocity shear layer thickness to density thickness.

Holmboe's results show the existence of the region of C_r=0 and the neutral curve at low α, as our results do. In Fig.6 J_0 is the Richardson number defined using the thickness of the transition layer of velocity profile as the characteristic scale and has the relation $J_0=R_i/2$.

On the other hand, Hazel defined the Richardson number J using the thickness of transition layer of density profile as the characteristic scale; therefore, we can not directly compare our results with his results. Then, we try to deduce a relation between J and R_i from the relations

$$\rho_1\approx\bar{\rho}e^{-\sigma/R}\ (y\to+\infty),\quad \rho_2\approx\bar{\rho}e^{\sigma/R}\ (y\to-\infty)$$
$$1-\gamma=1-\frac{\rho_1}{\rho_2}=1-e^{-2\sigma/R},\quad \sigma=-\frac{R}{2}\log\gamma\approx\frac{R}{2}(1-\gamma) \tag{21}$$

Finally we obtain the relation as follows;

$$J\equiv\frac{\sigma gh}{V^2}\approx\frac{R\varepsilon gh}{2V^2}=\frac{R}{2}R_i \tag{22}$$

and hence the neutral curve at low α, represented approximately by $J=R\alpha$, becomes $R_i=2\alpha$ in the (α, R_i) plane. This agrees with the results of our model corresponding to the case of $R\to\infty$ in Hazel's model (note that the agreement of this with the results for Kelvin-Helmholtz flow is only at $R_i\to 0$). However, Hazel's numerical results for stationary unstable modes, namely the modes of C_r=0, are different not only from Holmboe's results but also from our results. If the stationary neutral curve remains within the range of $J<1/4$, *i.e.* $R_i<1/2R$ in the (α, R_i) plane, the region under the curve is reduced as R increases, and finally disappears at $R\to\infty$ in the (α, R_i) plane. Moreover, if the maximum value of J for stationary unstable modes increases as R increases, and indicates a constant value not in the (α, J) plane but in the (α, R_i) plane at limit of $R\to\infty$, that is, if the maximum value of J increases in proportion to the value of R, Hazel's result is consistent with other results. Now calculating the largest value of R_i for stationary unstable modes from Hazel's results, J approximately equals 0.37, and we get R_i=0.15. This value agrees well with ours. We therefore conclude that the region of stationary unstable modes in Holmboe's or our results corresponds to the region bounded by the locus of bifurcation points (line *c* in Fig.8 of Hazel's paper) and the stationary neutral curve (line *e*) in Hazel's results.

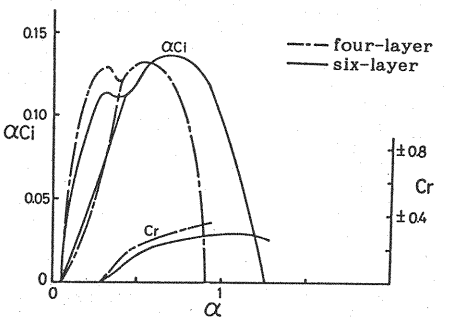

Fig.8 Phase velocity and growth rate for J_0=0.05

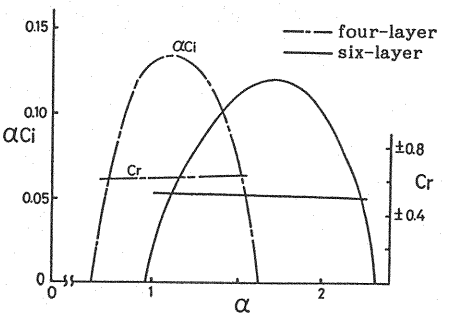

Fig.9 Phase velocity and growth rate for J_0=0.5

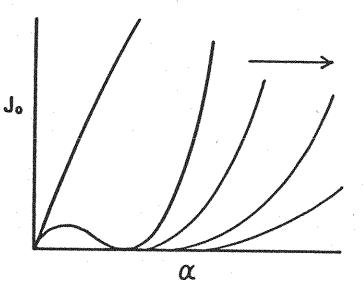

Fig.10 Sketch of change of a neutral curve as the number of layers of velocity profile increases

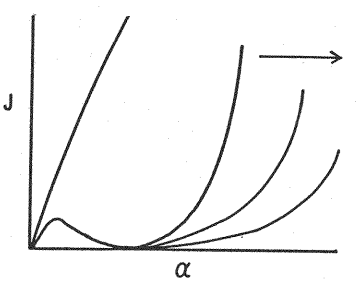

Fig.11 Sketch of change of a neutral curve as the thickness of transition layer of density profile decreases

The above discussions concern neutral curves at low α and for stationary unstable modes. As shown in Figs.6 and 7, Holmboe and Hazel also obtained neutral

curves at high α in their models, but in our model, no neutral curve at high α has been obtained. In order to discuss the appearance of this instability boundary, we have investigated the instability of a six-layer model with linear velocity profile in each layer and with a density gap at y=0, which has more layers than Holmboe's and is a better approximation of hyperbolic-tangent velocity profile. Figures.8 and 9 show αC_i and C_r for these two models. The results show that the unstable region has a tendency to expand to the high α domain, though the neutral point at low α and the region C_r=0 coincides with Holmboe's model. If the number of layers is increased further, *i.e.* the velocity profile approaches a smooth curve, the unstable region will expand further to high α, as shown in Fig.10. Accordingly, for a tanh-type profile corresponding to the case of infinite division, the unstable region does not seem to promise to disappear at any high value of α. We therefore conclude that the appearance of the neutral curve at high α obtained by Holmboe is due to the fact that the velocity profile is linear, *i.e.* the vorticity profile is discontinuous. Such a stabilization in high α due to linear modeling of velocity profile is also found by Miles & Howard[7] for stratified flow and by Esch[3] for homogeneous flow.

On the other hand, Hazel's results for the flow without an abrupt change in density profile show that the neutral curve appears in high α when R exceeds 2, although the velocity profile is a smooth curve. From the continuity of stability characteristics, we can expect the unstable region to expand to high α as R increases, as shown in Fig.11, and for the case of $R\to\infty$ the unstable region does not promise to close at any high α. We can therefore conclude that the appearance of the neutral curve in high α obtained by Hazel is due to the existence of a density transition layer, namely the continuity of density profile.

Though the neutral curves in high α obtained by Hazel and Holmboe strongly resemble each other as Hazel points out, the internal details are quite different. If we increase the number of layers in Holmboe's model or reduce the thickness of density transition layer in Hazel's model, we will obtain the same stability characteristics as our model in either case.

In this paper, our calculations were based on an assumption of inviscid flow; for the viscid flow case, we can expect to obtain neutral curves closed in the (α,R_i) plane due to the stabilizing effect of viscosity. In fact, such neutral curves have been obtained for several Reynolds numbers by numerical analysis (see Nishida & Yoshida[8]).

CONCLUSIONS

The linear stability analysis of inviscid two-layer flow with a hyperbolic-tangent velocity profile leads to the following conclusions:

(1) The neutral curve is represented by approximately R_i=2 α in the (α,R_i) plane and the unstable region spreads to high values of α.

(2) There is a region of stationary unstable modes at low R_i.

(3) The stationary neutral curve shown by Hazel is not found.

(4) The appearance of the neutral curve at high α obtained by Holmboe is due to linear modeling of velocity profile, *i.e.* discontinuity of vorticity profile.

(5) The appearance of the neutral curve at high α obtained by Hazel is due to the existence of a density transition layer, *i.e.* continuity of density profile.

REFERENCES

1. Bateman, H. : Higher Transcendental Functions, Vol.3, McGraw-Hill Book Company, 1955.
2. Drazin, P.G. and L.N. Howard : Advances in Applied Mechanics, Vol.9, Academic Press, New York, pp.1-89, 1966.
3. Esch, R.E. : The stability of a shear layer between two parallel streams, J. Fluid Mech., Vol.3, pp.289-303, 1957.
4. Hazel, P. : Numerical studies of the stability of inviscid stratified shear flows, J. Fluid Mech., Vol.55, pp.39-61, 1972.
5. Holmboe, J. : On the behavior of symmetric waves in stratified shear layers, Geophys. Publ., Vol.24, pp.67-113, 1962.

6. Michalke,A. : On the inviscid instability of the hyperbolic-tangent velocity profile, J. Fluid Mech., Vol.19, pp.543-556, 1964.
7. Miles, J.W. and L.N. Howard : Note on a heterogeneous shear flow, J. FluidMech., Vol.20, pp.331-336, 1964.
8. Nishida, S. and S. Yoshida : Stability and eigenfunctions of stratified two-layer shear flow, Third International Symposium on Stratified Flows(1987), Reidel Publishing Co., Dordrecht, (in press).
9. Thorpe, S.A. : Experiments on the stability of stratified shear flows: miscible fluids, J. Fluid Mech., Vol.46, pp.299-319, 1971.
10. Tominaga, M. : Kaiyo-hado (Ocean Wave), Kyoritu Press, Tokyo, 1976.
11. Turner, J.S. : Buoyancy Effect in Fluids, Cambridge University Press, Cambridge, 1973.

APPENDIX - NOTATION

The following symbols are used in this paper:

C = dimensionless complex phase velocity;

C_i = imaginary part of dimensionless complex phase velocity;

C_r = real part of dimensionless complex phase velocity;

g = gravitational acceleration;

i = imaginary unit;

J = Richardson number defined by Hazel;

J_o = Richardson number defined by Holmboe;

l = characteristic length;

R = ratio of velocity and density scales;

R_i = Richardson number defined in the present study;

U = dimensionless velocity profile;

U^* = velocity profile;

V = characteristic velocity;

x = dimensionless horizontal coordinate;

y = dimensionless vertical coordinate;

y^* = vertical coordinate;

α = dimensionless wavenumber;

γ = density ratio;

ε = relative density difference;

ρ_1 = density of upper layer fluid;

ρ_2 = density of lower layer fluid;

ϕ_1 = dimensionless stream function of disturbance in upper layer; and

ϕ_2 = dimensionless stream function of disturbance in lower layer.